Supporting Information

Selective and Sensitive determination of capsaicin using Polymelamine formaldehyde decorated over carbon nanotubes

Daisy Mehta [a], Neha Thakur [a] and Tharamani C. Nagaiah [a] *

[a.] Department of Chemistry Indian Institute of Technology Ropar Rupnagar, Punjab-140001, India.

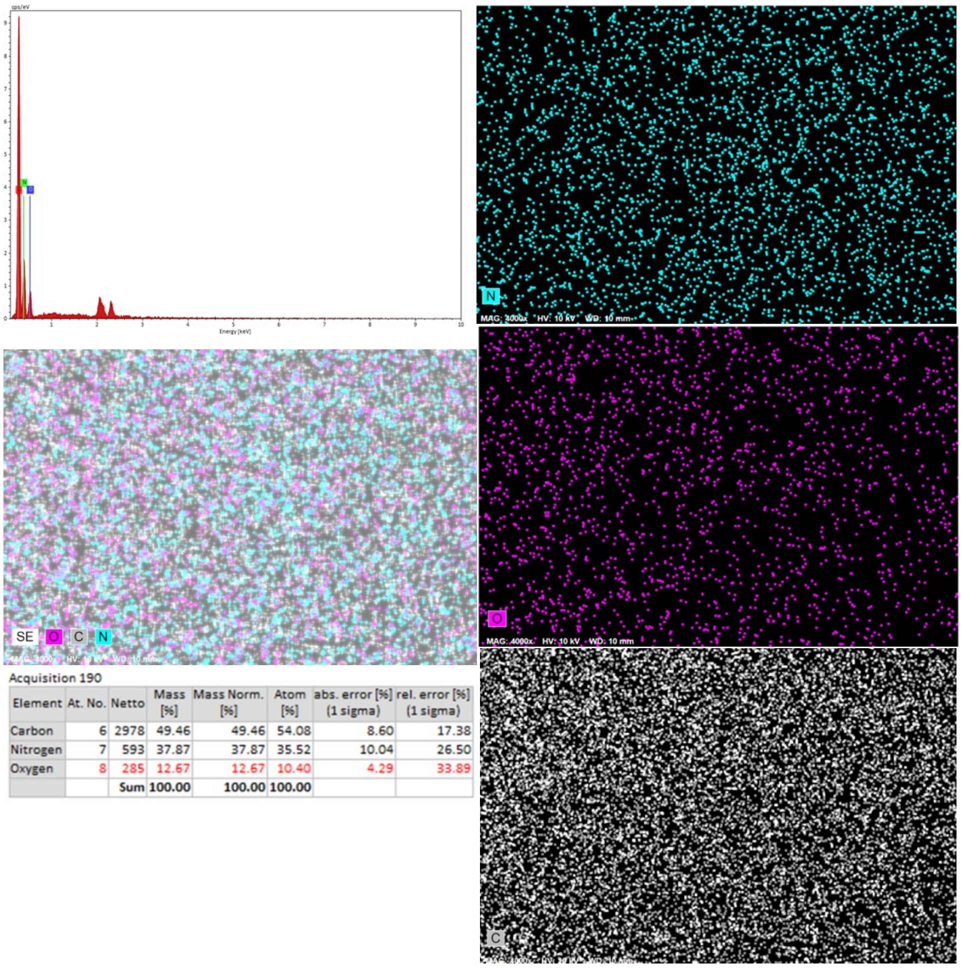

Acquisition 190

Element	At. No.	Netto	Mass [%]	Mass Norm. [%]	Atom [%]	abs. error [%] (1 sigma)	rel. error [%] (1 sigma)
Carbon	6	2978	49.46	49.46	54.08	8.60	17.38
Nitrogen	7	593	37.87	37.87	35.52	10.04	26.50
Oxygen	8	285	12.67	12.67	10.40	4.29	33.89
		Sum	100.00	100.00	100.00		

Figure

S1. (a)

EDS dot mapping of different elements present in PMF/OCNT composite.

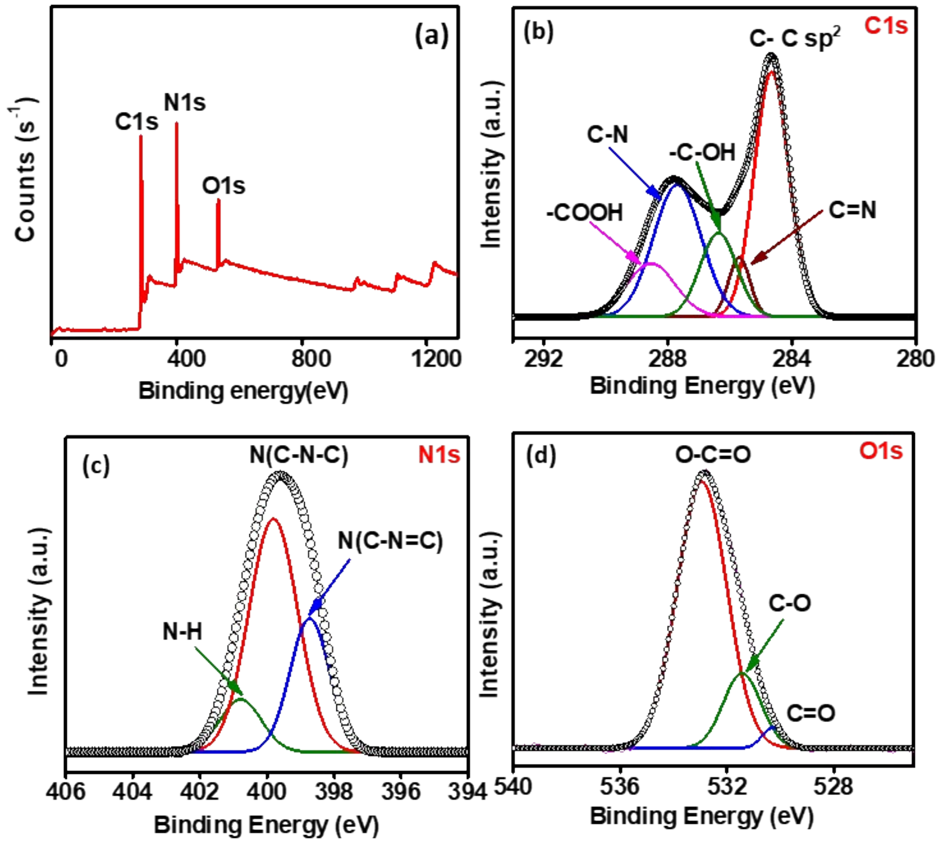

Figure S2. (a) XP survey spectra and deconvoluted XP spectra of (b) C1s (c) N1s (d) O1s of PMF/OCNT composite.

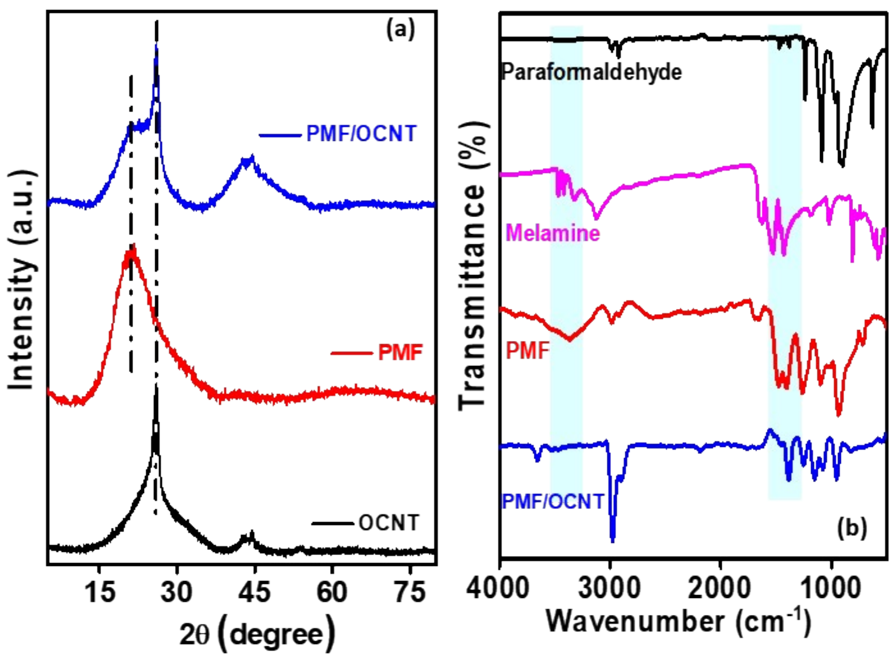

Figure S3. (a) XRD pattern of PMF, OCNTs and PMF/OCNT composite (b) FTIR spectra of PMF and melamine and PMF/OCNT composite.

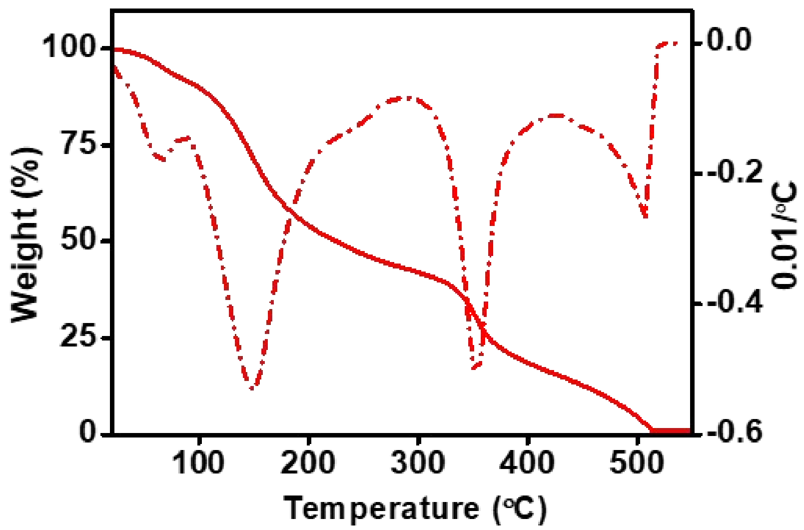

Figure S4. TGA curve and 1st derivative showing the weight loss of paraformaldehyde.

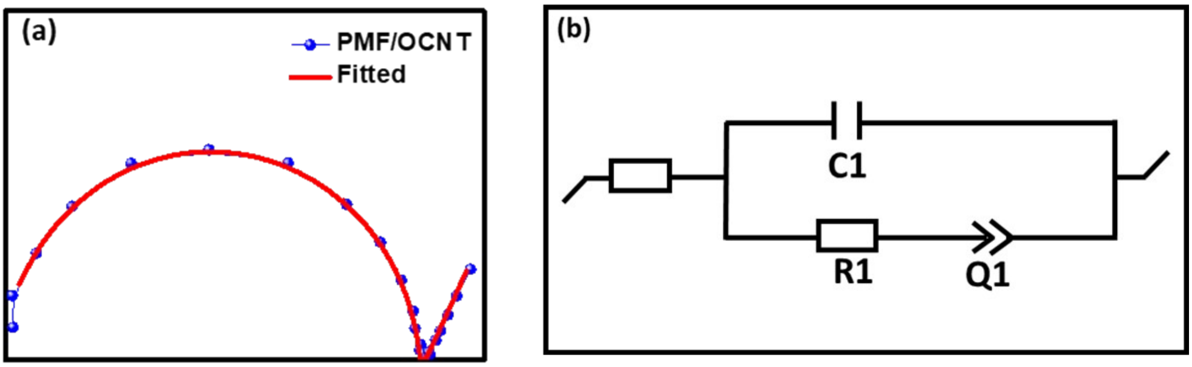

Figure S5. (a) Fitted EIS for PMF/OCNT (b) Corresponding equivalent circuit

Table S1: Charge transfer resistance extracted from EIS spectra.

Material	R_{ct}
Bare	283
PMF	182
PMF/OCNT	123

Electrochemical surface area (ECSA)

Electrochemically active surface area of the catalyst was determined by calculating the double-layer pseudo-capacitance (C_{dl}) in the non-faradaic region in 50 mM BR buffer with an analyte solution. CV was performed in non-faradic region/double-layer region in potential range from 0.00 V to 0.40 V *vs.* Ag/AgCl/3 M KCl at various scan rates (25 to 350 mV s^{-1}). The slope of the plot between averaged current density of anodic and cathodic current (Ia+Ic)/2 (where, ‘a’ denotes anodic current and ‘c’ is for cathodic current) *vs*. the scan rate at 0.199 V *vs.* Ag/AgCl/3 M KCl gives pseudo capacitance was dividing with the specific capacitance (Cs) of the flat standard surface (20-60 µF cm^{-2}), which is considered to be 40 µF cm^{-2}, gives electrochemical surface area (ECSA).

ECSA = $\boldsymbol{C_{dl}}$ / $\boldsymbol{C_s}$

Table S2: Electrochemical surface area (ECSA) analysis.

Sample	Catalyst	C_{dl} (μF) at 0.199 V *vs.* Ag/AgCl	ECSA (cm^2)
1.	PMF	2200	32.5 cm^2
2.	PMF/OCNT	1300	50 cm^2

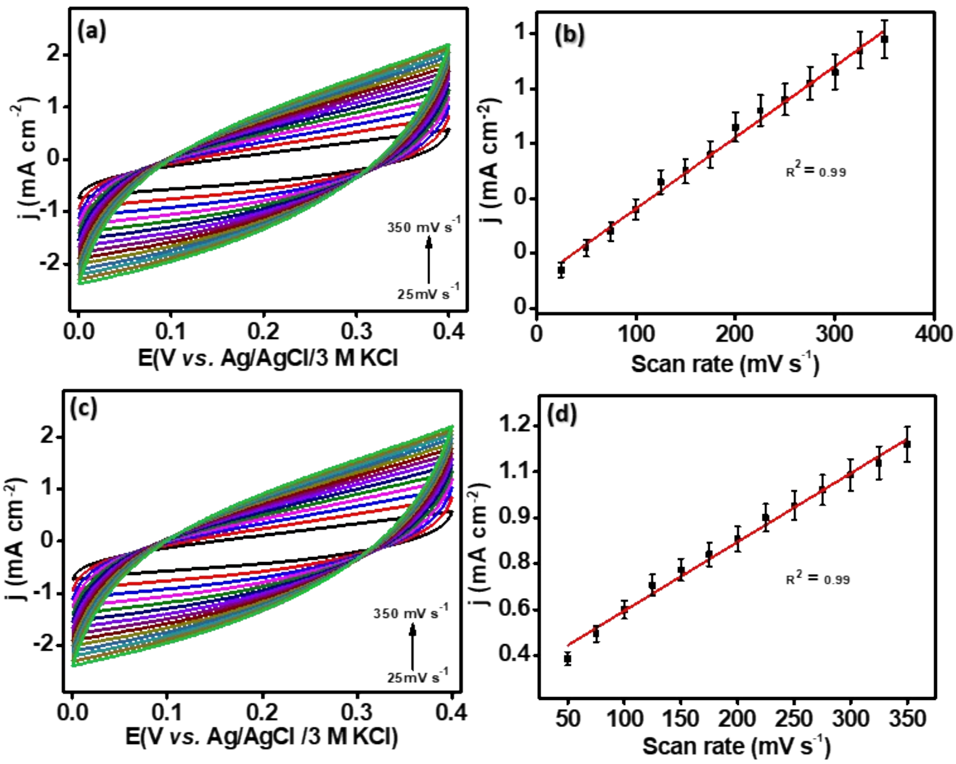

Figure S6. (a) & (c) Cyclic voltammograms of PMF and PMF/OCNT composite at varying scan rates in the non-faradic potential region and (b)&(d) corresponding average current densities respectively *vs.* scan rate at varying scan rates ranging from 25 to 350 mVs^{-1}.

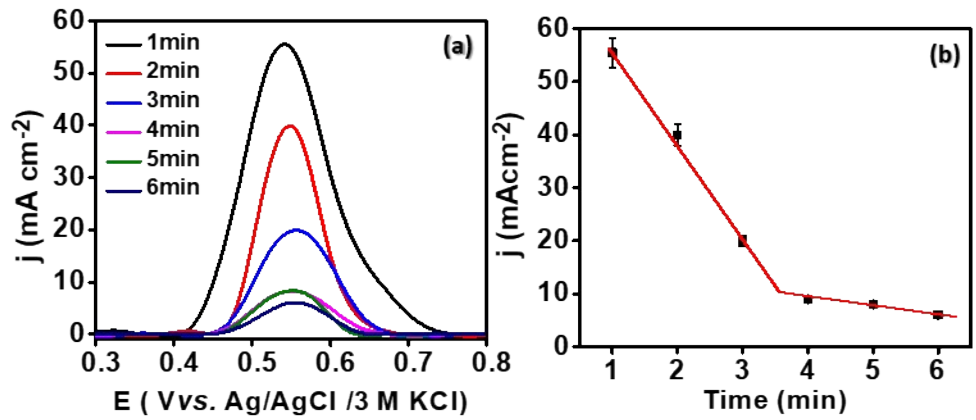

Figure S7. (a) SWV of for PMF/OCNT composite in 50 mM of BR Buffer(pH-1) containing 100 µM capsaicin. (b) corresponding calibration curve.

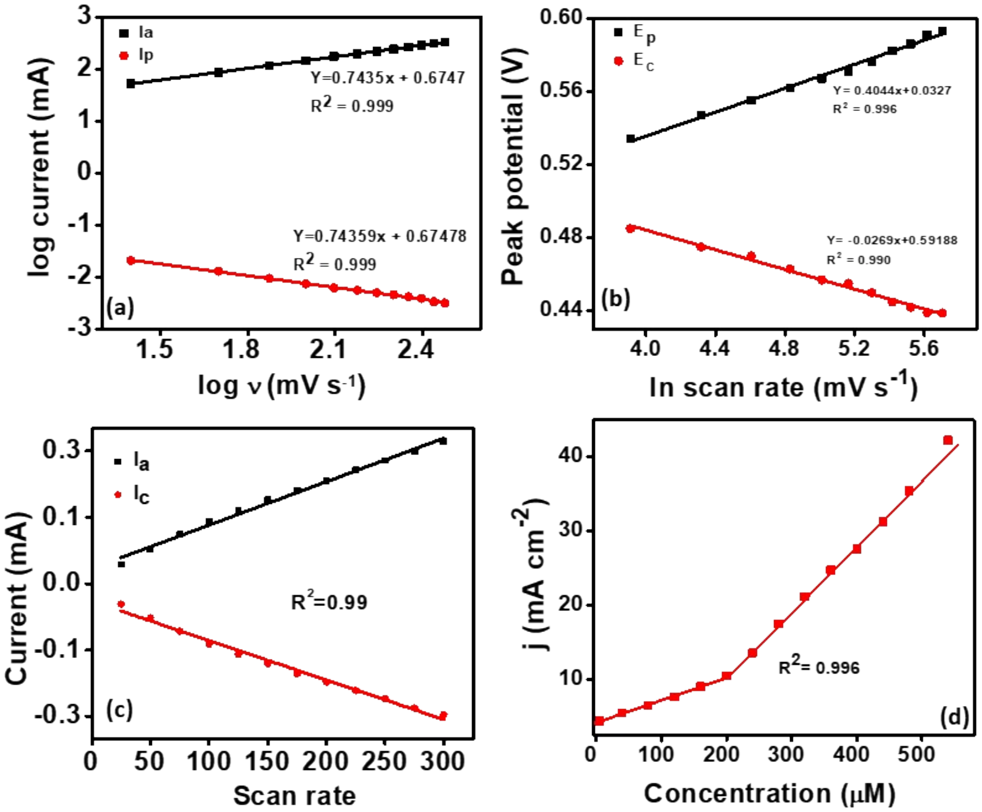

Figure S8. (a) Plot for Oxidation/Reduction peak current against the logarithm of scan rate (b) Plot for Oxidation/Reduction peak potential against the logarithm of scan rate plot for Oxidation/Reduction Peak current in 50 mM BR buffer (pH 1.0) containing 100 µM Capsaicin(c) calibration plot of peak current vs scan rate at varying scan rates extracted from cyclic voltammogram (Fig. 3f) (d) Calibration plot of current density and concentration of capsaicin for PMF/OCNT composite extracted from cyclic voltammogram (Fig. 4b).

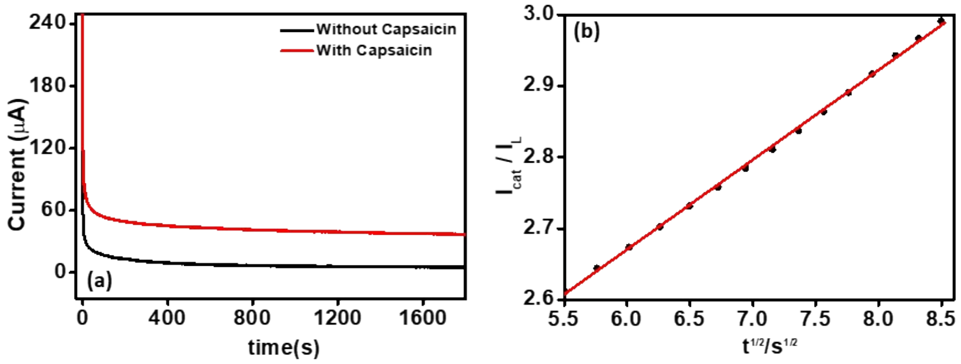

Figure S9. (a) Chronoamperometric curves of PMF/OCNT composite in BR buffer (pH 1.00) with and without 100 µM capsaicin and (b) plot of I_{Cat}/I_L vs. $t^{1/2}$ from the chronoamperometric curves.

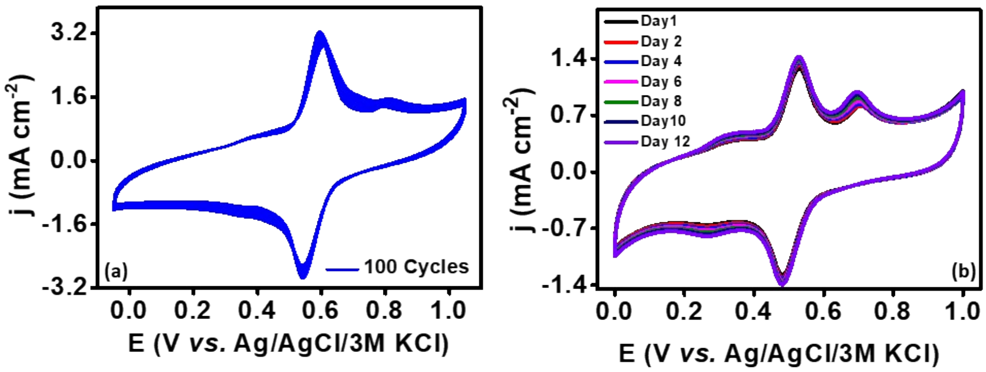

Figure S10. Cyclic voltammogram showing (a) stability of PMF/OCNT composite over continuous 100 cycles (b) Long term storage stability of sensor towards electrooxidation of capsaicin in 50 mM BR buffer pH 1.0 containing 100 µM of capsaicin at a scan rate of 50 mV s^{-1}.

Table S3. Comparison of analytical performance of PMF/OCNT composite towards capsaicin detection with the previously reported literature.

Electrode	Detection Method	Linear Range (µM)	Lowest Detection Limit (µM)	Sensitivity (mA µM^{-1} cm^{-2})	Literature
MWCNT/BPPGE	ADsSV	0.5-15 & 15-60	0.31	-	1
BDD	ADsSV	0.16-20	0.034	-	2
NH_2-FMS	LSV	0.04-0.40 & 0.40-4.0	0.020	-	3
MCFs	DPV	0.76-11.65	0.08	-	4
GO/Ti/Nafion	LSV	0.03-10.0	0.0086	-	5
PAL/ Nafion/MWCNTs	DPV	20-100	0.61	-	6
EDI-SPE	LSV	5-100 µM	2.88		7
HRP/SPE	Chronoamperometry	0.75-25	0.30	-	8
Ppy/Bi_2O_3	SWV	0.26-2.6	0.059	-	9
CNTs/RuNPs	SWV	0.010-0.41	0.41	-	10
Mn-SeNP	DPV	5.0-128	0.050	2.41 µA µM^{-1} cm^{-2}	11
Unmodified SPE	DPV	0.16-16	0.050	-	12
TiO_2 NPs	CV	6.0-75 & 12-138	5.34 & 11.3	-	13
Y_2O_3 NPs	DPV	1.0 & 80	-	-	14
PDDA/rGO/Pd	CV, DPV	0.32-64	0.10	-	15
IL/ rGO/Nafion	LSV	0.030-10	0.0032	-	16
Sn/rGO	CV	0.2-22	0.005	-	17
10% CB	DPV	0.080-60	0.028		18
N-doped GrNPs	DPV	1-100	0.37	-	19
Pencil Graphite	AdsSV	0.016-0.32	0.0037	-	20
β-CD/CPE	AdSV	1.3-9.3	0.21	-	21
Fe^{III}-HMOF-5	CV, DPV	1-60	0.4	-	22
$Ru(bpy)_3^{2+}$	CV	0.01-100	0.094	-	23
PMF/OCNT	**CV, SWV, EIS**	**0.1-240 & 240-500**	**0.071 & 0.085**	**960 µA µM cm^{-2} & 2900 µA µM cm^{-2}**	**This work**

Table S4. Determination of Capsaicin in different real samples using PMF/OCNT composite.

Sample	Analyte	Actual conc.	Conc. (added)	Conc. (found)	SHU	Recovery (%)
Fresh Green Pepper	Capsaicin	102 µM	100 µM	216 µM	1055	114
Belle Pepper	Capsaicin	70 µM	70 µM	139.5 µM	681	99.2
Cayenne pepper	Capsaicin	54 µM	50 µM	109.4 µM	534	110

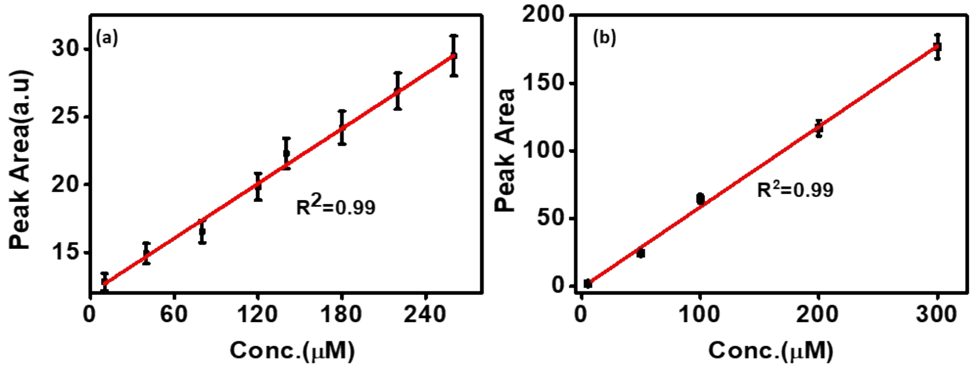

Figure S11. Calibration curve between concentration and peak area with (a) Electrochemical method (b) HPLC after the addition of standard sample of capsaicin .

Table S5. Comparison of results obtained by electrochemical method with HPLC for real sample.

Sample	Analyte	Electrochemical method conc.(µM)	HPLC conc.(µM)	Relative Error (%)
Fresh Green Pepper	Capsaicin	216 µM	230 µM	6.09 %
Belle Pepper	Capsaicin	139 µM	143 µM	4%
Cayenne pepper	Capsaicin	109 µM	106 µM	-3%

References

1. R. T. Kachoosangi, G. G. Wildgoose and R. G. Compton, *Analyst*, 2008, **133**, 888-895.
2. Y. Yardım, *Electroanalysis*, 2011, **23**, 2491-2497.
3. Y. Ya, L. Mo, T. Wang, Y. Fan, J. Liao, Z. Chen, K. S. Manoj, F. Fang, C. Li and J. Liang, *Colloids Surf .B.*, 2012, **95**, 90-95.
4. Z. Xue, C. Hu, H. Rao, X. Wang, X. Zhou, X. Liu and X. Lu, *Anal. Methods*, 2015, **7**, 1167-1174.
5. D.-H. Kim and W.-Y. Lee, *J. Electroanal. Chem.*, 2016, **776**, 74-81.
6. M. I. Sabela, T. Mpanza, S. Kanchi, D. Sharma and K. Bisetty, *Biosens. Bioelectron.*, 2016, **83**, 45-53.
7. G. D. Pierini, C. W. Foster, S. J. Rowley-Neale, H. Fernández and C. E. Banks, *Analyst*, 2018, **143**, 3360-3365.
8. R. Mohammad, M. Ahmad and L. Y. Heng, *Sens. Actuators B: Chem.*, 2017, **241**, 174-181.
9. A. Verma and R. Jain, *J. Electrochem. Soc.*, 2017, **164**, H908.
10. A. K. Baytak and M. Aslanoglu, *Food Chem.*, 2017, **228**, 152-157.
11. R. Sukanya, M. Sakthivel, S.-M. Chen, T.-W. Chen, F. M. Al-Hemaid, M. A. Ali and M. S. Elshikh, *Microchimica Acta*, 2018, **185**, 1-9.
12. W. Lyu, X. Zhang, Z. Zhang, X. Chen, Y. Zhou, H. Chen, H. Wang and M. Ding, *Sens. Actuators B: Chem.*, 2019, **288**, 65-70.
13. M. Sarma and M. del Valle, *Electroanalysis*, 2020, **32**, 230-237.
14. H. Naskar, B. Ghatak, S. Biswas, B. Tudu, R. Bandyopadhay and P. Pramanik, 2019.
15. F. Zhong, Z. Liu, Y. Han and Y. Guo, *Electroanalysis*, 2019, **31**, 1182-1188.
16. D.-H. Kim, S. Nam, J. Kim and W.-Y. Lee, *J. Electrochem. Sci. Technol*, 2019, **10**, 177-184.
17. W. Numphud, O. Chienthavorn and W. Siriwatcharapiboon, *Sci. Asia*, 2020, **46**, 586-+.
18. P. B. Deroco, O. Fatibello-Filho, F. Arduini and D. Moscone, *Electrochim. Acta*, 2020, **354**, 136628.
19. A. Soleh, K. Saisahas, K. Promsuwan, P. Thavarungkul, P. Kanatharana and W. Limbut, *ACS Appl. Nano Mater.*, 2020, **3**, 10094-10104.
20. Y. Yardım and Z. Şentürk, *Talanta*, 2013, **112**, 11-19.
21. Q. Gu, C. Lu, K. Chen, X. Chen, P. Ma, Z. Wang and B. Xu, *Foods*, 2021, **10**, 1743.
22. X. Fang and R. Duan, *Frontiers in chemistry*, 2022, **10**.
23. S. J. Lee and W.-Y. Lee, *J. Electroanal. Chem.*, 2022, 116169.